Numerical Simulations of 1461 and 1762 San Pio delle Camere (L'Aquila) Earthquakes Using 3D Physic-Based Model

Donato Pera[1(✉)], F. Di Michele[2], E. Stagnini[3], B. Rubino[1], R. Aloisio[3,4], and P. Marcati[3]

[1] Department of Information Engineering, Computer Science and Mathematics, University of L'Aquila, via Vetoio, loc. Coppito, I, L'Aquila, Italy
donato.pera@univaq.it
[2] Istituto Nazionale di Geofisica e Vulcanologia, via Alfonso Corti 12, Milan, Italy
[3] Gran Sasso Science Institute (GSSI), via M. Iacobucci 2, L'Aquila, Italy
[4] INFN-Laboratori Nazionali del Gran Sasso, Via G. Acitelli 22, Assergi, AQ, Italy

Abstract. The aim of this paper is to propose a physics-based simulation of the two earthquakes that hit the surrounding area of the city of L'Aquila (Abruzzo central Italy) in 1461 and 1762, with magnitudes 6.4 Mw and 6.0 Mw, respectively. Both events are placed, by the available literature, on the fault structure named San Pio delle Camere [11]. The physical parameters characterizing the earthquake such as fault plane, epicenter, and magnitude are considered to be fixed. Starting from them three stochastic rupture scenarios are generated from each earthquake using three different slip distributions. The scenarios were evaluated in relation to the possibility to reproduce the macroseismic intensity field available from the historical catalogs. The simulated values of peak velocity are used to derive the value of the macrosiesmic intensity obtained by a suitable empirical relationship specifically derived for Italy.

For the numerical simulations we used a three-dimensional soil model used and validated in a previous study related to the 2009 L'Aquila earthquake. The considered slip distributions are able to reproduce quite well the macroseismic effect of the 1461 earthquake. While none of the three scenarios developed satisfactorily reproduce the 1762 earthquake.

1 Introduction

Abruzzo (central Italy) is a region of high seismic risk, having been hit by numerous earthquakes in the past, the most recent in 2009 [7,20]. For many of them, however, which occurred in the pre-instrumental era, available information are often lacking and/or inaccurate. Therefore physical based (PB) numerical simulations represent a valuable tool to increase the understanding of the area, both from a geological and historical point of view.

The 27th November 1461 and 6th October 1762 earthquakes, object of this study, are just two of the several seismic events that hit L'Aquila in the past. Both of them, according to the available literature, were caused by the San Pio delle Camere fault system [11].

© The Author(s), under exclusive license to Springer Nature Switzerland AG 2023
O. Gervasi et al. (Eds.): ICCSA 2023 Workshops, LNCS 14111, pp. 549–565, 2023.
https://doi.org/10.1007/978-3-031-37126-4_35

In addition to historical interest, this work may be useful in assessing the effect of future earthquakes that may occur on the same fault. Before analysing the results of the simulation we shortly introduce the two events, summarising the (few) available information.

According to the available literature, the 1461 earthquake had epicenter at Lat 42.314-Lon 13.5429 and estimated magnitude 6.4 Mw. As reported in the *Catalogo dei forti terremoti in Italia 461A.C.-1997 e dell'area mediterranea 760A.C-1500* from mid-November 1461 to the end of March 1462, the area of the Abruzzo Apennines, where L'Aquila was one of the most important cities, was hit by a sequence of earthquakes. On November 16, 1461, a shock was felt in L'Aquila which did not cause any damage. A few days later, on the night of 27 November, preceded by strong underground noises, two strong tremors struck the L'Aquila area. These earthquakes seriously affected all the buildings in the city of L'Aquila: a quarter of the houses collapsed entirely and all the others suffered partial collapses and very serious injuries. The north-western area of the city was the most damaged with about 75 houses destroyed. The north-eastern area of the city was less damaged than the others. Many of the very numerous towers of the city also collapsed. For the city of L'Aquila it is possible to have a detailed list of damage to churches and public buildings in the urban area. According to chronicle sources, 46 monuments in the city were hit. There were collapses, partial collapses, or damage to churches and bell towers, monasteries, palaces and hospitals. The dead were numerous: about 80 or 100 depending on the sources, many of whom were overwhelmed by the collapse of the vaults of the main hospital (S.Salvatore). The effects of the earthquake were worsen by fire and, later, by the abundant snowfalls that occurred in January 1462. In the area surrounding L'Aquila, made up of a total of over 80 fortified villages, the following were seriously affected: Onna (I_{MCS} 10), where all the houses collapsed causing the death of many of the inhabitants; Sant'Eusanio Forconese (I_{MCS} 10) which was almost entirely destroyed, including the recently built castle, there were many victims. The Castelnuovo (I_{MCS} 9.5) village collapsed almost entirely, including the towers of the walls and there were 28 dead. The Castelvecchio Calvisio (I_{MCS} 9) suffered the collapse of many houses and there were 12 dead, also Poggio Picenze (I_{MCS} 9) collapsed almost entirely. This earthquake was felt without damage in a very large area in particular in other cities as Perugia and Rome. On December 11, 1461, the most intense phase of the seismic sequence ended, up to that day, about a hundred seismic events were felt in L'Aquila.

The 1762 earthquake had an estimated epicenter at Lat 42.308 Lon 13.585 and moment magnitude Mw 6.0. Also for this second earthquake, we can report the description of *Catalogo dei forti terremoti in Italia 461A.C.-1997 e dell'area mediterranea 760A.C-1500*. According to it, the main shock occurred on 6 October 1762 around 13 o'clock "Italian" time and violently struck two villages near L'Aquila, named Castelnuovo (I_{MCS} 9.5) and Poggio Picenze (I_{MCS} 9), causing the total or partial collapse of most of the houses. Many buildings suffered the fall of the roofs or the untying of the load-bearing walls, described by witnesses

as irreparably damaged and on the verge of falling. The general condition of the two villages, which emerges from the detailed contemporary sources, is that of two almost completely uninhabitable sites. The earthquake was strongly felt in the nearby towns of Barisciano (I_{MCS} 4.5) and San Demetrio ne' Vestini (I_{MCS} 4.5), where no damage is reported finally in L'Aquila (I_{MCS} 7), where it caused injuries and caused chimneys to fall. This earthquake was felt lightly also in Rome.

Recently, massive technological advances related to the development of High Performance Computing (HPC) technologies [42] have made it possible to simulate complex earthquake events at local and regional scales [1,3,12,13,15,34,41,48]. In the last decades, Physical Based Simulations (PBS) techniques have been extensively used to simulate earthquakes that occurred in the recent past [13,15,34,47], but limited efforts have been devoted to the numerical reconstruction of historical earthquakes for which no recordings are available. As an example, in [32] a stochastic finite-fault method model is applied to simulate the 1939 Erzincan Earthquake (Ms 7.8). The model has validated comparing the computed macroseismic intensity, obtained according to [10], with those provided by the historical catalogs. Moreover some plausible scenarios of the 1895 Ljubljana earthquake are presented in [52].

Within this paper numerical simulations are performed using a numerical simulation tool named SPEED based on the Discontinuous Galerkin Spectral Element Method [36] (http://speed.mox.polimi.it). As we say before for both the earthquakes we are considering, the epicenter is probably located on the San Pio delle Camere fault. However the related slip distribution is obviously unknown. To overcome this problem we use a suitable tool for stochastic slip distribution generation, derived according to [31] and actually embedded on SPEED.

We consider three different realizations of the slip distributions for both the 1461 and 1762 earthquakes. Then the PGV values, provided by each simulations, are employed to get an estimate of the macroseismic intensity (I_{MCS}) value using the empirical model recently proposed by [37]. The simulated values of the I_{MCS} are then compared with those made available by the CFTI5Med and CPTI15 catalogs [27,28,45,46]. More details that we use for the comparison of I_{MCS} values of 6 villages for 1461 earthquake and 5 villages for the 1762 events are reported as in Table 3 and 4. We just point out as only the villages located inside our computational domain are considered.

The paper is organized as follows. In Sect. 2 we briefly describe the workflow related to the construction of the computational domain, the mathematical formulation of the problem and empirical model employed to correlate PGV and MCS intensities. In Sect. 3 we present and discuss our results. Finally, in the last section, we summarize our conclusions and present some possible developments of this study.

2 Computational Model and Mathematical Tools

Seismic waves propagation during seismic events are influenced by geological structures such as alluvial basins, passive fault structures, and cavities as well as by the topography and the human constructions (see eg., [8,12,14,22,29,33,43,44,53] and references therein). The goal of a PBS model is to get seismic ground shaking scenarios that are realistic and sufficiently close to seismic records, when they are available. For this purpose, it is essential to have an accurate *digital twin* of the studied seismic area, which requires geophysical information that are not always available. Luckily for the earthquakes related to this work thanks to the work of *Microzonazione sismica* of Central Italy, realized by the *Protezione Civile italiana* after the 2009 L'Aquila earthquake, a large amount of data are available, according to this collected data a reconstruction of the geological stratigraphy of the subsoil is possible. Our computational domain extends about 67.2 km × 59.7 km in the East-West and North-South directions respectively and for 20.1 km in depth. The horizontal layered crustal model contains four layers with different thicknesses as in [13,15], the thickness and the mechanical properties for each earth-crust layer are reported in Table 1. To account for the local application, we also include a detailed three dimensional reconstruction of the quaternary L'Aquila - San Demetrio sedimentary basin (see Fig. 2) validated in [13].

Fault	Mesh Features	Domain Image
L=16.2 Km W=10.5 Km Strike=127° Dip=50° Rake=270°	Size=(67.2,59.7,20.1Km N. Elements=1660440 Spectral Degree=3 N. Mesh Nodes=1838615 Δt=0.0003s Duration=30s	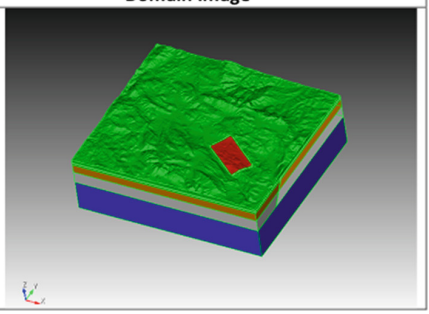

Fig. 1. In the first two columns we report the main characteristics of the fault plane and the computational domain. In the last column, we show a 3D representation of the computational domain, the projection of the fault zone in the top surface (green color) is highlighted in red. (Color figure online)

According to [15], the velocity and the quality factor inside the basin are modelled using a depth-dependent profile as follows:

$$V_S = 300 + 36 \cdot z^{0.43}(\mathrm{m/s}),\ V_P = V_S\sqrt{4.57},\ Q_S = 0.10V_S, \tag{1}$$

whereas the density is constant: $\rho = 1.9(\mathrm{g/cm^3})$.

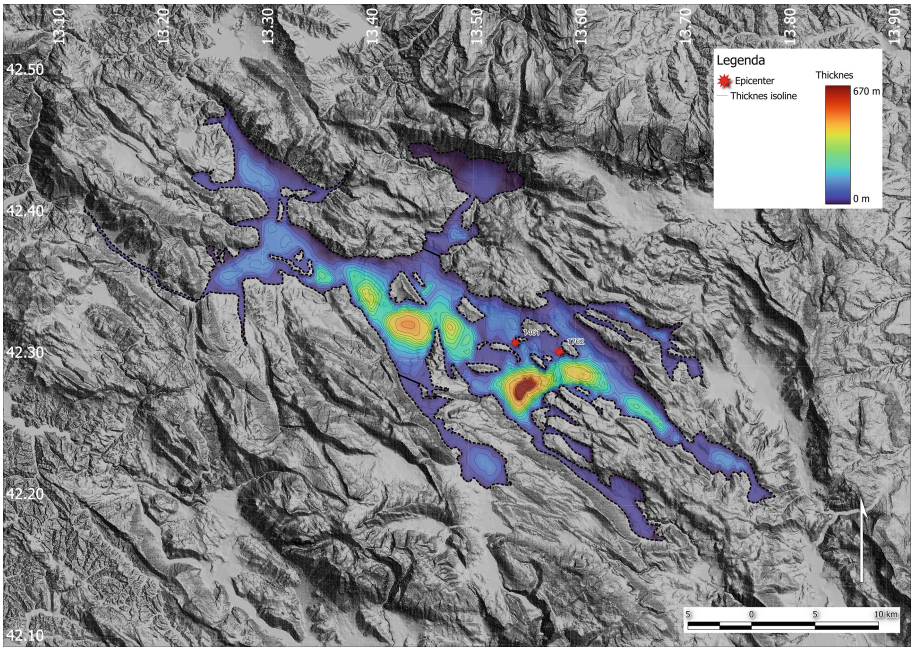

Fig. 2. Map of the Quaternary L'Aquila - San Demetrio sedimentary basin (geological model available as in [13]). The observed microcosmic intensity, according to the CFTI5Med catalogue, and the position of the epicenter are also reported

Table 1. Mechanical properties of the crustal layers.

Layer	*Depth*(km)	V_S(m/s)	V_P(m/s)	ρ(g/cm^3)	Q_S
1	0–1	1700	3160	2.5	100
2	1–2	2600	4380	2.5	200
3	2–5	3100	5760	2.84	200
4	5–20	3500	6510	3.18	200

The topography that forms the surface layer of our model has been realized using the python tool introduced in [35], starting from a dataset made available by the project TINITALY [49–51]. The seismogenic fault plane corresponding to the fault of San Pio delle Camere, has been constructed according to the database DISS (Database of Individual Seismogenic Sources) [9]. This fault plane has dimensions of 16.2 km in length and 10.5 km in width, whereas strike, dip, and rake angles are respectively 127°, 50° and 270° (cf. Fig. 1).

The position of the hypocenters are obtained using epicenter position and fault geometry. We got respectively $z_{hypo} = 6.16$ km for the 1461 earthquake and $z_{hypo} = 4.38$ km for the 1762 earthquake. The computational domain is meshed using *CUBIT* (https://coreform.com/products/coreform-cubit/) getting $1.66 \cdot 10^6$ elements, having a size ranging from 130 m (top layer) to max 1 Km (bottom layer).

From the mathematical point of view the computational domain is modelled as a polygonal bounded domain $\Omega \subset \mathbb{R}^3$ with outward pointing normal unit $\mathbf{n}$. The domain boundary is decomposed into three disjoint surfaces, with names Γ_D, Γ_N and Γ_A. On each considered surfaces we assign the displacement, traction, and fictitious traction values respectively. The fictitious traction is needed to prevent non physical reflections on the boundaries, whereas on Γ_N we prescribe free surface conditions.

The displacement at the soil level $\mathbf{u}(\mathbf{x}, t) = (u_1, u_2, u_3)(\mathbf{x}, t)$ will be described, for the values $t \in [0, T]$ and $\mathbf{x} \in \Omega$, as

$$\rho \partial_{tt}^2 \mathbf{u} + 2\rho\xi\partial_t \mathbf{u} + \rho\xi^2 \mathbf{u} - \nabla \cdot \sigma(\mathbf{u}) = \mathbf{f}, \tag{2}$$

where $\mathbf{f}$, $\rho = \rho(\mathbf{x}) > 0$ and σ are the external applied load, the mass density and the stress tensor respectively. We define the stress tensor as a function of the displacement using the formula:

$$\sigma_{ij} = \mu \left(\frac{\partial u_i}{\partial x_j} + \frac{\partial u_j}{\partial x_i} \right) + \lambda \sum_{k=1}^{3} \frac{\partial u_k}{\partial x_k} \delta_{ij}, \quad \text{for } i, j = 1, 2, 3 \tag{3}$$

where δ is the Kronecker symbol. The positive and bounded functions $\lambda = \lambda(\mathbf{x})$ and $\mu = \mu(\mathbf{x})$ are the first and second Lamé coefficients, respectively. Whereas ξ always defined in (2) is a decay factor $\xi = \xi(x) > 0$ that models the viscosity of the media [6] and has dimension $[1/sec]$. In this work, this parameter has been defined using an a-dimensional quality factor $Q = Q_0 f / f_0$ where f_0 is a reference frequency and $Q_0 = \pi f_0 / \xi$.

The boundaries conditions are defined as: $\mathbf{u} = \mathbf{0}$ on Γ_D, $\sigma\mathbf{n} = \mathbf{0}$ on Γ_N, $(\sigma\mathbf{n})^* = \mathbf{0}$ on Γ_A. We refer to [6] for the complete definition of $(\sigma\mathbf{n})^*$.
We set $\mathbf{u}(\mathbf{x}, 0) = \mathbf{0} \quad \partial_t \mathbf{u}(\mathbf{x}, 0) = \mathbf{0}$ as initial condition. We report also the useful formula to compute the *compressional* and *shear* wave velocities from the Lamé coefficients and the mass density.

$$V_P = \sqrt{(\lambda + 2\mu)/\rho} \qquad V_S = \sqrt{\mu/\rho}.$$

For the body force distribution $\mathbf{f}$ we consider $\mathbf{f}(\mathbf{x}, t) = \nabla \cdot \mathbf{m}(\mathbf{x}, t)$, as in [17], where $\mathbf{m}(\mathbf{x}, t)$ is the seismic moment tensor as reported in [2]. The method used to approximate equation (2) is the spectral element method in space coupled with the leap-frog scheme in time according to SPEED software tool used in this work [36]. Finally for the stability and convergence of the used numerical method we refer to [4,5,21]. We refer also to [30,38–40,47] for other interesting applications in computational seismology. Using the mentioned above mathematical model and computational domain we performed for each seismic event three numerical simulations named as scenario 1,2 and 3 (SC1, SC2 and SC3 in the following). For each simulated scenario we generate a stochastic slip distributions as reported in Fig. 3, using the basic geophysical parameters reported above. The considered simulation time for each scenario it is equal to 30 s with

a time step $\Delta t = 0.0003\,\mathrm{s}$ (see Fig. 1). All numerical simulations have been executed in the Linux High Performance Computing cluster Caliban located in the High-Performance Computing Laboratory of the Department of Information Engineering, Computer Science and Mathematics (DISIM) at the University of L'Aquila. Each single simulation ran using 128 MPI processes on DELL PowerEdge C6400-4-blades-C6525 servers equipped with 2x CPU AMD EPYC 7282 2.7GHz and 128GB Ram per blade. As mentioned above each used server is located inside the DISIM Caliban HPC cluster based on Rocks Cluster 7.0 (Manzanita) (http://www.rocksclusters.org/). The computational time required for a single run it is equal to 34 h (run-time execution).

After running simulations, for each scenario it is necessary to derive the relative values of I_{MCS} to compare with available historical data.

In the literature, different empirical relationships have been proposed to correlate the macroseismic intensity I_{MCS} with selected ground-motion intensity measures, such as peak ground velocity and peak ground acceleration. Models specific designed and validate for the Italian territory had been, for example, proposed in [16,18,23,24]. They are based on the statistical fitting of data from past earthquakes, and are very useful to estimate the damage due to past or potential future earthquakes, although it is recognized that they suffer high uncertainties.

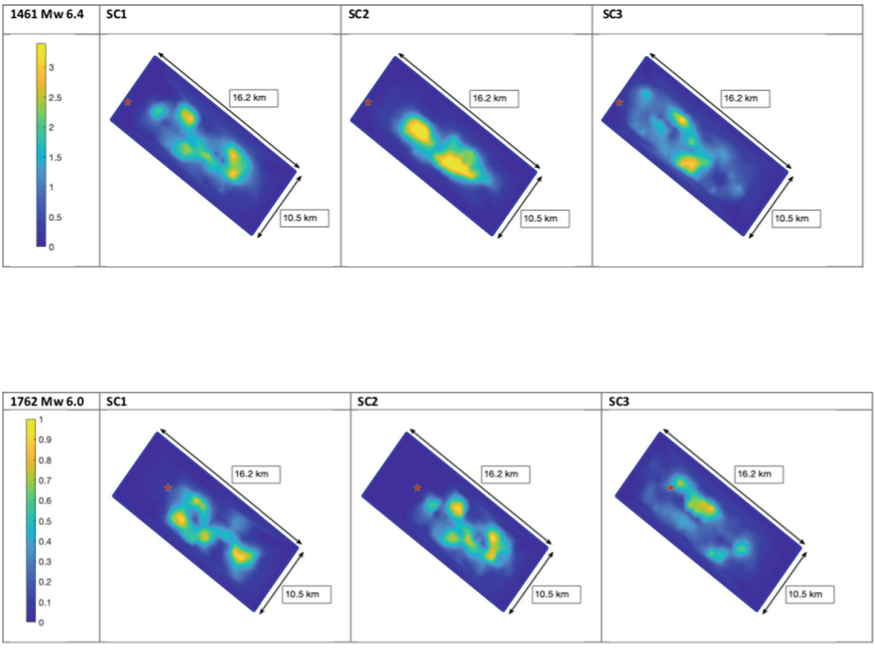

Fig. 3. Slip distributions provided by the rupture model generator introduced by [31] and available in the SPEED pre-processing tool, for the four hypothetical earthquake scenarios considered in this study for the 1461 Mw6.4 (top) 1762 earthquake Mw 6.0 (bottom.)

Among the many empirical relationships available in the literature, here we will consider the most recent model proposed in [37]. In this paper, the authors correlate peak ground velocity (PGV), peak ground acceleration (PGA) and spectral acceleration (SA) at 0.3, 1.0 and 3.0 s with the macroseismic intensity (I_{MCS}). Both the European Macroseismic (EMS-98) and the Mercalli-Cancani-Sieberg (MCS) scales are considered. The (invertible) relations are derived using the orthogonal distance regression technique, already applied for a similar purpose in [18,19]. The working dataset contains earthquakes that occurred in Italy between 1972 and 2016 and a quadratic correlation between the intensity and the base-10 logarithm of I_{MCS} has been considered, instead of the linear one often employed in other studies.

In other words, the authors assume

$$I = a + b \log_{10} I_{MCS} + c(\log_{10} I_{MCS})^2, \tag{4}$$

where the coefficients a,b, and c are derived for each couple of the dependent-independent variables.

For the purpose of this paper we just consider the relation linking microcosmic intensity in the Mercalli-Cancani-Sieberg scale ad PGV reported in Table 2. In fact, the frequency resolution of the model is 2 Hz, which is not sufficient to ensure accurate estimation of PGA and spectral acceleration values.

Table 2. Available relationships between the macroseismic intensity, expressed in MCS scale, and peak ground velocity (PGV) according to [37]

Model	PGV
Oliveti et al. (2022) [37]	$I_{MCS} = 4.31 + 1.99 * \log_{10} PGV + 0.58 + (\log_{10} PGV)^2$

3 Results and Discussion

In this section we present and discuss our result. For each scenario we calculate the PGV as the geometric average of the horizontal components, and then the I_{MCS} using the model proposed in [37]. In particular we focus on the location listed in Table 3 and 4, for which the values of the I_{MCS} are available for comparison from the historical catalogues.

In Tables 5 and 6 we report for each scenario a comparison among the CFT15Med and the simulated macrosiesmic intensity values. In more details Table 5 refers to the 1461 event whereas Table 6 is related to 1762 event. Both the historical and estimate I_{MCS} are reported. In the column named *Err* we report, for each scenario, the difference between the simulated value and the historical one.

As mentioned in the introduction, the 1461 and 1762 seismic events were felt by the population and certainly caused damage to the buildings. According

Table 3. Macroseismic intensity in MCS scale for the 1461 earthquake related to 6 towns included in the computational domain. In the last two columns the geographical coordinates and the distance from the estimated epicenter are reported.

I_{MCS}	Name	Lat-Lon	Epicentral Distance (km)
X	Onna (AQ)	42.328–13.479	5.5
X	San'Eusanio Forconese (AQ)	42.288–13.524	3.3
IX-X	Castelnuovo (AQ)	42.295–13.628	7.3
IX	Castelvecchio Calvisio (AQ)	42.311–13.688	11.9
IX	L'Aquila (AQ)	42.356–13.396	13.0
IX	Poggio Picenze (AQ)	42.321–13.541	0.8

Table 4. Macroseismic intensity in MCS scale for 1762 earthquake related to 5 towns included in the computational domain. In the last two columns the geographical coordinates and the distance from the estimated epicenter are reported.

I_{MCS}	Name	Lat-Lon	Epicentral Distance (km)
IX-X	Castenuovo (AQ)	42.295–13.628	3.8
IX	Poggio Picenze (AQ)	42.321–13.541	3.9
VII	L'Aquila (AQ)	42.356–13.396	16.4
IV-V	Barisciano (AQ)	42.326–13.592	2.1
IV-V	San Demetrio ne' Vestini (AQ)	42.289–13.558	3.1

Table 5. Macroseismic intensity in MCS scale for the 6 towns included in the computational domain comparison between estimated and simulated data earthquake 1461.

Name	I_{MCS}	I_{MCS} SC1	I_{MCS} SC2	I_{MCS} SC3	ErrSC1	ErrSC2	ErrSC3
Onna	10	8.60	7.65	8.68	−1.39	−2.35	−1.32
Sant'Eusanio Forconese	10	8.85	8.3	8.61	−1.14	−1.69	−1.39
Castelnuovo	9.5	11.10	10.02	11.46	1.60	0.52	1.96
Castelvecchio Calvisio	9	10.53	8.56	8.86	1.53	−0.43	−0.14
L'Aquila	9	7.28	6.34	6.82	−1.72	−2.66	−2.17
Poggio Picenze	9	9.77	8.51	8.92	0.77	−0.48	−0.08

to the CFT15Med Catalogue the 1461 seismic event had I_{MCS} with a range from 9 to 10 with the maximum (10) in Onna (AQ) and Sant'Eusanio Forconese (AQ). While the 1762 earthquake had I_{MCS} with a range from 4.5 to 9 with the maximum (9) in Castelnuovo.

To get a quantitative measure of the performance of each scenario and understand which one provides better results, we introduce the two metrics described below

$$E_{max} = \max |I_{MCS}(i) - I_{MCS,real}(i)|, \tag{5}$$

Table 6. Macroseismic intensity in MCS scale for the 5 towns included in the computational domain comparison between estimated and simulated data earthquake 1762.

Name	I_{MCS}	I_{MCS} SC1	I_{MCS} SC2	I_{MCS} SC3	ErrSC1	ErrSC2	ErrSC3
Castenuovo	9.5	7.81	8.84	8.03	−1.69	−0.66	−1.47
Poggio Picenze	9.0	5.78	6.55	6.98	−3.22	−2.45	−2.02
L'Aquila	7	4.82	5.65	5.57	−2.18	−1.35	−1.43
Barisciano	4.5	6.20	7.46	6.54	1.7	2.96	2.04
San Demetrio ne' Vestini	4.5	7.65	8.68	8.47	3.15	4.18	3.97

$$E_{mean} = E_{tot}/N \quad \text{where} \quad E_{tot} = \sum_{i=1}^{N=k} |I_{MCS}(i) - I_{MCS,real}(i)|\,, \tag{6}$$

where $I_{MCS}(i)$ and $I_{MCS,real}(i)$ are, respectively, the ith value I_{MCS} of the calculated using [37] and provided by the catalogue CFT15Med. Here $k = 6$ and $k = 5$ for 1461 and 1762 seismic event, respectively. The values of the maximum error (5) and the mean error (6) are displayed in Tables 7, for both the considered seismic events. Point values of damage calculated at specific sites are necessary for model evaluation and validation. The advantage of physical-based simulations is that they provide detailed information about the entire area affected by the earthquake, taking into account the geology and topography of the area. Simulations, in other words, can be useful to supplement, refute and validate available historical data. Therefore for both the earthquakes we also analyze the spatial distribution of the macroseismic intensity obtained and the PGV for the best scenario.

Table 7. Maximum and average errors on the evaluation of the I_{MCS} using PGV for the IM models and the scenario for 1461 and 1762 events

	SC1		SC2		SC3	
	E_{max}	E_{mean}	E_{max}	E_{mean}	E_{max}	E_{mean}
1461	1.72	1.36	2.66	1.35	2.17	1.18
1762	3.22	2.39	2.96	2.32	3.97	2.19

Figure 4 shows the maps PGV obtained using best score scenario for the 1461-SC1 in (a) and 1762-SC2 in (b). The PGV has been calculated as the geometric mean of the maximum horizontal component obtained from the numerical simulations.

Figure 5 shows the I_{MCS} maps obtained from PGV values using the scenarios with a lower average error, for the 1461-SC1 in (a) and 1762-SC2 in (b).

From the PGV and I_{MCS} maps we can see as for both the considered seismic events we got the highest values in the south-east region of the alluvional basin.

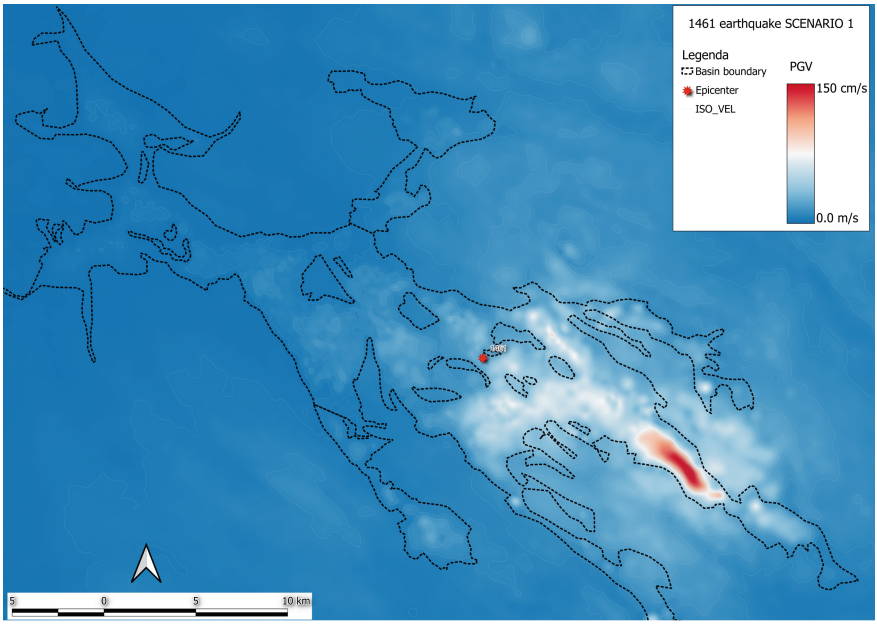

(a) $PGVSC1 - 1461$

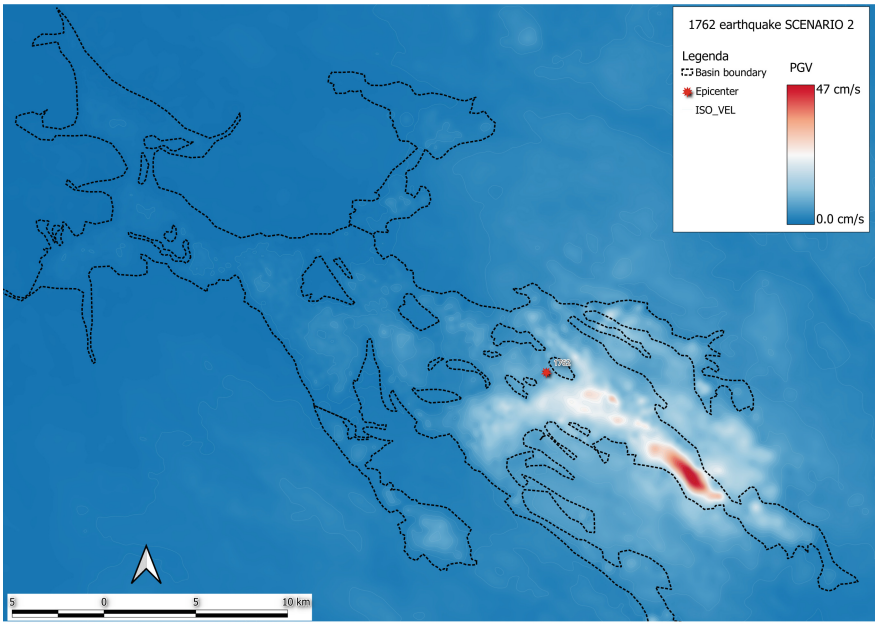

(b) $PGVSC2 - 1762$

Fig. 4. PGV maps: peak ground velocity maps calculated using the best scenario, namely SC1 for 1461 (a) and SC2 for 1762 (b). In both cases, the peak velocity in correspondence with the southeastern region of the alluvial basin

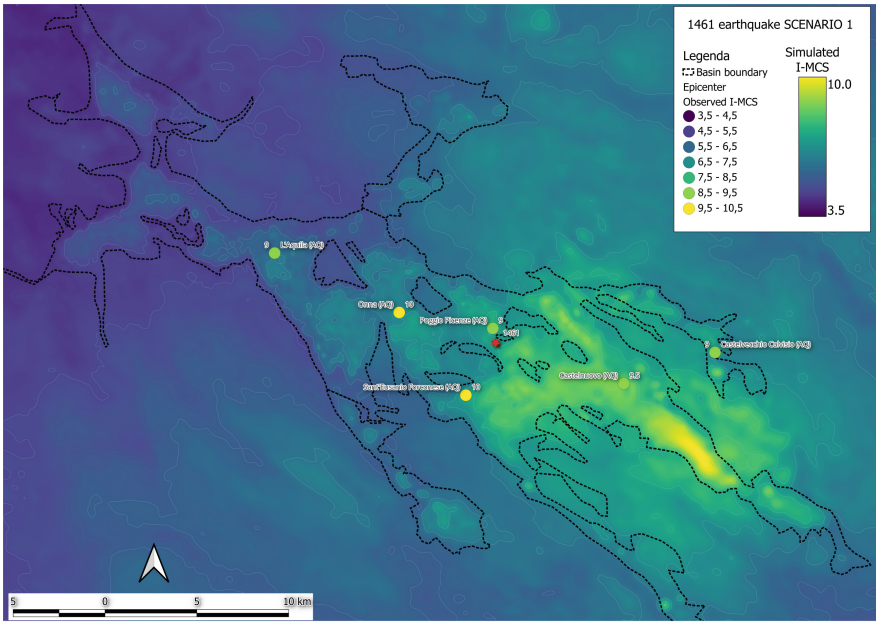

(a) I_{MCS} SC1-1461

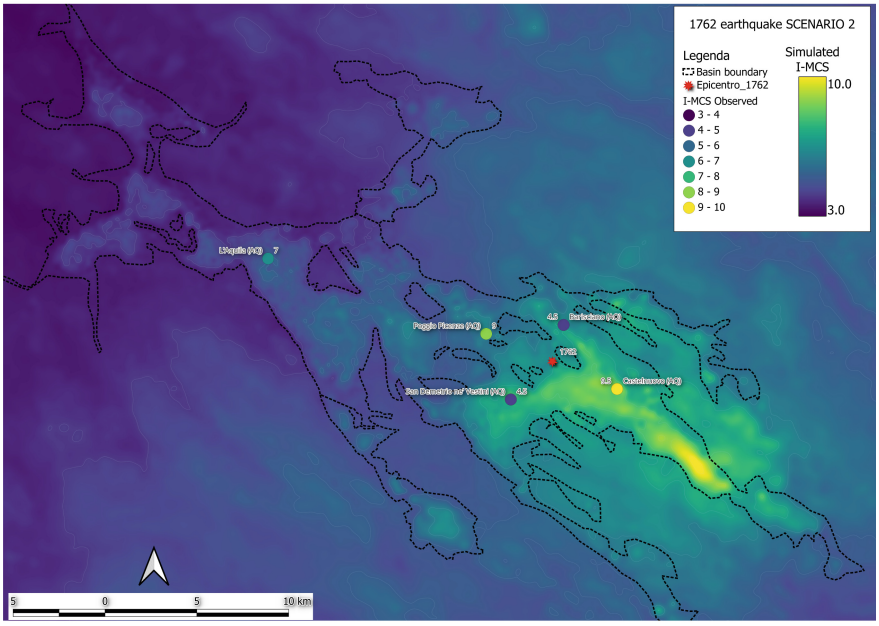

(b) I_{MCS} SC2-1762

Fig. 5. Microcosmic Intensity maps: I_{MCS} obtained starting from the best score scenario namely SC1 for 1461(a) and SC2 for 1762 (b).

This behavior is probably due to the superposition of two effects. On the one hand, in this region between present-day San Pio delle Camere and Navelli, there is a local maximum in the thickness of the sedimentary basin (see Fig. 2), which amplifies the seismic signal. On the other hand, the slip distributions corresponding to SC1 for 1461 and SC2 for 1762 (Fig. 3) show a peak in the in the south zone of the fault structure in correspondence with the PGV peak observed in Fig. 4. In more detail analyzing both the maps and the relative errors, we can say that for the 1461 earthquake: SC2 appears to be the worst scenario. SC1 and SC3 have a quite satisfactory behaviour in all considered villages with the best fitting data in Poggio Picenze and the wrost in L'Aquila city. SC1 shows a good agreement between the real and simulated data also in the part of the domain where the other scenarios fail. Finally for the all scenarios we got the wrost results in L'Aquila and Onna locations. Although all scenarios acceptably reproduce the considered seismic event, according to the previous analysis, we can conclude that the best scenario is SC1, having the highest slip distribution in the south region of the fault. The less accurate results are instead provided by SC2, for which the maximum asperity path is located in the central part of the fault structure. For the 1762 earthquake: SC3 appears to be the worst scenario. SC1-SC2 also doesn't have in general a quite satisfactory behaviour also if we are able to get good results in Castelnuovo location. SC2 shows the best agreement between the real and simulated data with the best results in Castelnuovo and the wrost in San Demetrio dei Vestini. Finally we found that all scenarios fail in reproducing the damage in San Demetrio dei Vestini and Poggio Picenze locations. Therefore according to the previous analysis, we can conclude that the best scenario among the three considered is SC2, having the highest slip distribution in the central-south region of the fault. The less accurate results are instead provided by SC3, for which the maximum asperity path is located in the north part of the fault structure. In general, however, none of the scenarios satisfactorily reproduce this event.

4 Conclusions

In this article, we present some plausible scenarios for two earthquakes occurring in the Aterno valley region on 27 November 1461 and 6 October 1762. We reconstructed a computational domain with an extends of 67.2 km × 59.7 km in the East-West and North-South directions respectively and for 20.1 km in depth centered in L'Aquila city and realized using the CUBIT Coreform meshing tool. For both the simulated earthquakes each scenario has been simulated using SPEED tool with fixed values of Magnitude (6.4 Mw and 6.0 Mw for 1461 and 1762, respectivetly), fault plane and epicenter, but different slip distributions. For each scenario, we computed the PGV values and then the I_{MCS} using the model available from the literature defined in [37]. Among the available simulations SC1 better reproduce the 1461 earthquake. It is characterized by a localized slip distribution in the south part of the fault structure, which could be a plausible slip distribution for the 1461 earthquake. Concerning the 1762, no scenario

can satisfactorily reproduce the (few) information available. However the SC2, characterized by a localized slip distribution in the central-south part of the fault structure, is the one that shows better performance. In summary, we can say that the 1461 earthquake is acceptably reproduced by all slip distributions considered, whereas the results are less satisfactory for 1762. Although three scenarios are few to draw conclusions, it is possible to assume that the available information is not sufficient and/or accurate enough to model this event. It is in our opinion necessary to develop a more accurate analysis that not only considers more scenarios, but also investigates the location of the epicenter and possibly the fault structure. Finally, we recall the lack of other reconstructions relating to the simulation of the earthquakes considered in this article and the possibility of extending the domain reconstruction and earthquake simulation techniques to other historical earthquakes for the definition and study of risk plans related to the Italian territory. Some other simulations based in the same area are available on platform https://www.opendatalaquila.it, together with much other information about the L'Aquila area and the reconstruction process after the 2009 earthquake, [25,26].

Acknowledgements. This paper is part of a larger project focused on the post-earthquake reconstruction of the city of L'Aquila (see https://www.opendatalaquila.it) and was partially supported by the GSSI "Centre for Urban Informatics and Modelling" (CUIM). This paper received financial support from ICSC - Centro Nazionale di Ricerca in High Performance Computing, Big Data and Quantum Computing, funded by European Union - NextGenerationEU (ref. Prof. B. Rubino and Dr. D. Pera. University of L'Aquila). All numerical simulations have been realized on the Linux HPC cluster Caliban of the High Performance Parallel Computing Laboratory of the Department of Information Engineering, Computer Science and Mathematics (DISIM) at the University of L'Aquila.

References

1. Abraham, J.R., Smerzini, C., Paolucci, R., Lai, C.G.: Numerical study on basin-edge effects in the seismic response of the Gubbio valley, central Italy. Bull. Earthquake Eng. **14**(6), 1437–1459 (2016)
2. Aki, K., Richards, P.G.: Quantitative seismology (2002)
3. Antonietti, P.F., et al.: Three-dimensional physics-based earthquake ground motion simulations for seismic risk assessment in densely populated urban areas. Math. Eng. **3**(2), 1–31 (2021). https://doi.org/10.3934/mine.2021012, https://www.aimspress.com/article/doi/10.3934/mine.2021012
4. Antonietti, P.F., Ayuso de Dios, B., Mazzieri, I., Quarteroni, A.: Stability analysis of discontinuous Galerkin approximations to the elastodynamics problem. J. Sci. Comput. **68–1**, 143–170 (2016)
5. Antonietti, P.F., Mazzieri, I., Quarteroni, A., Rapetti, F.: Non-conforming high order approximations of the elastodynamics equation. Comput. Meth. Appl. Mech. Eng. **209**, 212–238 (2012)
6. Antonietti, P., et al.: Numerical modeling of seismic waves by discontinuous spectral element methods. ESAIM: Proc. Surv. **61**(1–37) (2018)

7. Anzidei, M., et al.: Coseismic deformation of the destructive April 6, 2009 l'aquila earthquake (central Italy) from GPS data. Geophy. Res. Lett. **36**(17) (2009)
8. Baron, J., Primofiore, I., Klin, P., Vessia, G., Laurenzano, G.: Investigation of topographic site effects using 3D waveform modelling: amplification, polarization and torsional motions in the case study of arquata del tronto (italy). Bull. Earthquake Eng. **20**(2), 677–710 (2022)
9. Basili, R., et al.: Database of individual seismogenic sources (diss), version 3.3. 0: A compilation of potential sources for earthquakes larger than m 5.5 in Italy and surrounding areas (2021)
10. Bilal, M., Askan, A.: Relationships between felt intensity and recorded ground-motion parameters for turkey. Bull. Seismolog. Soc. Am. **104**(1), 484–496 (2014)
11. Boncio, P., Lavecchia, G., Pace, B.: Defining a model of 3D seismogenic sources for seismic hazard assessment applications: the case of central Apennines (Italy). J. Seismolog. **8**, 407–425 (2004)
12. Di Michele, F., et al.: On the possible use of the not-honoring method to include a real thrust into 3D physical based simulations. In: 2021 21st International Conference on Computational Science and its applications (ICCSA), pp. 268–275. IEEE (2021)
13. Di Michele, F., et al.: Spectral element numerical simulation of the 2009 L'aquila earthquake on a detailed reconstructed domain. Geophys. J. Int. **230**(1), 29–49 (2022)
14. Di Michele, F., et al.: Fault shape effect on SH waves using finite element method. J. Seismol. 1–21 (2022)
15. Evangelista, L., et al.: Physics-based seismic input for engineering applications: a case study in the Aterno river valley, central Italy. Bull. Earthq. Eng. **15**(7), 2645–2671 (2017)
16. Faccioli, E., Cauzzi, C.: Macroseismic intensities for seismic scenarios estimated from instrumentally based correlations. In: Proceedings of the First European Conference on Earthquake Engineering and Seismology, paper. No. 569 (2006)
17. Faccioli, E., Maggio, F., Paolucci, R., Quarteroni, A.: 2D and 3D elastic wave propagation by a pseudo-spectral domain decomposition method. J. Seismolog. **1**(3), 237–251 (1997)
18. Faenza, L., Michelini, A.: Regression analysis of MCS intensity and ground motion parameters in Italy and its application in Shakemap. Geophys. J. Int. **180**(3), 1138–1152 (2010)
19. Faenza, L., Michelini, A.: Regression analysis of MCS intensity and ground motion spectral accelerations (SAS) in Italy. Geophys. J. Int. **186**(3), 1415–1430 (2011)
20. Falcucci, E., et al.: The paganica fault and surface coseismic ruptures caused by the 6 April 2009 earthquake (L'aquila, central Italy). Seismol. Res. Lett. **80**(6), 940–950 (2009)
21. Ferroni, A., Antonietti, P.F., Mazzieri, I., Quarteroni, A.: Dispersion-dissipation analysis of 3-D continuous and discontinuous spectral element methods for the elastodynamics equation. Geophys. J. Int. **211–3**, 1554–1574 (2017)
22. Gao, Y., Zhang, N.: Scattering of cylindrical SH waves induced by a symmetrical v-shaped canyon: near-source topographic effects. Geophys. J. Int. **193**(2), 874–885 (2013)
23. Gomez Capera, A., Albarello, D., Gasperini, P., et al.: Aggiornamento relazioni fra l'intensità macrosismica e pga. progetto ingv-dpc s1, deliverable d11 (2007)
24. Gomez Capera, A., et al.: Macroseismic intensity to ground motion empirical relationships for Italy. In: Proceedings, vol. 37, pp. 289–291 (2018)

25. GSSI: Open data L'aquila (2019). https://www.opendatalaquila.it/
26. GSSI: Open data ricostruzione (2019). https://opendataricostruzione.gssi.it/home
27. Guidoboni, E., et al.: Cfti5med, the new release of the catalogue of strong earthquakes in Italy and in the Mediterranean area. Sci. Data **6**(1), 1–15 (2019)
28. Guidoboni, E., et al.: Cfti5med, catalogo dei forti terremoti in italia (461 ac-1997) e nell'area mediterranea (760 ac-1500) (2018)
29. Imperatori, W., Mai, P.M.: The role of topography and lateral velocity heterogeneities on near-source scattering and ground-motion variability. Geophys. J. Int. **202**(3), 2163–2181 (2015)
30. Infantino, M., Mazzieri, I., Özcebe, A.G., Paolucci, R., Stupazzini, M.: 3d physics-based numerical simulations of ground motion in Istanbul from earthquakes along the Marmara segment of the north Anatolian fault. Bull. Seismol. Soc. Am. **110–5**, 2559–2576 (2020)
31. J. Schmedes, R.J.A., Lavallée, D.: A kinematic rupture model generator incorporating spatial interdependency of earthquake source parameters (2013)
32. Karimzadeh, S., Askan, A.: Modeling of a historical earthquake in erzincan, turkey (ms˜ 7.8, in 1939) using regional seismological information obtained from a recent event. Acta Geophysica **66**(3), 293–304 (2018)
33. Lewis, M., Peng, Z., Ben-Zion, Y., Vernon, F.: Shallow seismic trapping structure in the san Jacinto fault zone near Anza, California. Geophys. J. Int. **162**(3), 867–881 (2005)
34. Magnoni, F., et al.: Spectral-element simulations of seismic waves generated by the 2009 L'aquila earthquake. Bull. Seismol. Soc. Am. **104**(1), 73–94 (2013)
35. May, J., Pera, D., Di Michele, F., Rubino, B., Aloisio, R., Marcati, P.: Fast cubit-python tool for highly accurate topography generation and layered domain reconstruction. In: 29th International Meshing Roundtable (2021)
36. Mazzieri, I., Stupazzini, M., Guidotti, R., Smerzini, C.: Speed: spectral elements in elastodynamics with discontinuous galerkin: a non-conforming approach for 3D multi-scale problems. Int. J. Numer. Meth. Eng. **95**(12), 991–1010 (2013)
37. Oliveti, I., Faenza, L., Michelini, A.: New reversible relationships between ground motion parameters and macrosesmic intensity for Italy and their application in shakemap. Geophys. J. Int. **231**(2), 1117–1137 (2022)
38. Paolucci, R., Evangelista, L., Mazzieri, I., Schiappaterra, E.: The 3D numerical simulation of near-source ground motion during the marsica earthquake, central Italy, 100 years later. Soil Dyn. Earthq. Eng. **91**, 39–52 (2016)
39. Paolucci, R., Mazzieri, I., Özcebe, A.G., Smerzini, C.: Anatomy of strong ground motion: near-source records and three-dimensional physics-based numerical simulations of the mw 6.0 2012 may 29 Po plain earthquake, Italy. Geophysical Journal International 203–3, 2001–2020 (2015)
40. Paolucci, R., Mazzieri, I., Piunno, G., Smerizni, C., Vanini, M., Özcebe, A.G.: Earthquake ground motion modeling of induced seismicity in the Groningen gas field. Earthquake Eng. Struct. Dyn. **50–1**, 135–154 (2021)
41. Paolucci, R., Evangelista, L., Mazzieri, I., Schiappapietra, E.: The 3d numerical simulation of near-source ground motion during the Marsica earthquake, central Italy, 100 years later. Soil Dyn. Earthq. Eng. **91**, 39–52 (2016)
42. Pera, D.: Design and performance evaluation of a Linux HPC cluster. Task Quart. **22**(2), 113–123 (2018)
43. Pilz, M., Parolai, S., Stupazzini, M., Paolucci, R., Zschau, J.: Modelling basin effects on earthquake ground motion in the santiago de chile basin by a spectral element code. Geophys. J. Int. **187**(2), 929–945 (2011)

44. Rodriguez-Plata, R., Ozcebe, A., Smerzini, C., Lai, C.: Aggravation factors for 2d site effects in sedimentary basins: the case of Norcia, central Italy. Soil Dyn. Earthq. Eng. **149**, 106854 (2021)
45. Rovida, A., Locati, M., Camassi, R., Lolli, B., Gasperini, P.: The Italian earthquake catalogue cpti15. Bull. Earthq. Eng. **18**(7), 2953–2984 (2020)
46. Rovida, A., Locati, M., Camassi, R., Lolli, B., Gasperini, P., Antonucci, A.: Catalogo parametrico dei terremoti italiani (cpti15). versione 4.0. Istituto Nazionale di Geofisica e Vulcanologia (INGV). Italy (2022)
47. Smerzini, C., Villani, M.: Broadband numerical simulations in complex near-field geological configurations: the case of the 2009 m w 6.3 L'aquila earthquake. Bull. Seismol. Soc. Am. **102**(6), 2436–2451 (2012)
48. Stupazzini, M., Infantino, M., Allmann, A., Paolucci, R.: Physics-based probabilistic seismic hazard and loss assessment in large urban areas: a simplified application to Istanbul. Earthquake Eng. Struct. Dyn. **50**(1), 99–115 (2021)
49. Tarquini, S., et al.: Tinitaly/01: a new triangular irregular network of Italy. Ann. Geophys. (2007)
50. Tarquini, S., Nannipieri, L.: The 10 m-resolution Tinitaly dem as a transdisciplinary basis for the analysis of the Italian territory: current trends and new perspectives. Geomorphology **281**, 108–115 (2017)
51. Tarquini, S., Vinci, S., Favalli, M., Doumaz, F., Fornaciai, A., Nannipieri, L.: Release of a 10-m-resolution dem for the Italian territory: Comparison with global-coverage Dems and anaglyph-mode exploration via the web. Comput. Geosci. **38**(1), 168–170 (2012)
52. Tiberi, L., Costa, G., Jamšek Rupnik, P., Cecić, I., Suhadolc, P.: The 1895 Ljubljana earthquake: can the intensity data points discriminate which one of the nearby faults was the causative one? J. Seismolog. **22**(4), 927–941 (2018)
53. Veeraraghavan, S., Coleman, J.L., Bielak, J.: Simulation of site and topographic effects on ground motion in los alamos, nm mesas. Geophys. J. Int. **220**(3), 1504–1520 (2020)